Strontium and cesium release mechanisms during unsaturated flow through waste-weathered Hanford sediments

Hyun-shik Chang [1,§], Wooyong Um [1,5,], Kenton Rod [1], R. Jeff Serne [1], Aaron Thompson [2], Nicolas Perdrial [3], Carl I. Steefel [4], and Jon Chorover [3]*

[1] Pacific Northwest National Laboratory, P.O. Box 999, Richland, WA 99354

[2] University of Georgia, Athens, GA 30602

[3] University of Arizona, Tucson, AZ 85721

[4] Lawrence Berkeley National Laboratory, Berkeley, CA 94720

[5] Pohang University of Science and Technology (POSTECH), South Korea

* CORRESPONDING AUTHOR: Wooyong Um. E-mail Wooyong.Um@pnl.gov, tel. 509.372.6227, fax. 509.376.4890; [§] Current address: Savannah River Ecology Laboratory, P.O. Drawer E, Aiken, SC, 29802. E-mail hchang@srel.edu, tel. 803.725.7351, fax. 803.725.7351

ABSTRACT

Leaching behavior of Sr and Cs in the vadose zone of Hanford site (WA, USA) was studied with laboratory-weathered sediments mimicking realistic conditions beneath the leaking radioactive waste storage tanks. Unsaturated column leaching experiments were conducted using background Hanford pore water focused on first 200 pore volumes. The weathered sediments were prepared by 6 months reaction with a synthetic Hanford tank waste leachate containing Sr and Cs (10^{-5} and 10^{-3} molal representative of LO- and HI-sediment, respectively) as surrogates for ^{90}Sr and ^{137}Cs. The mineral composition of the weathered sediments showed that zeolite (chabazite-type) and feldspathoid (sodalite-type) were the major byproducts but different contents depending on the weathering conditions. Reactive transport modeling indicated that Cs leaching was controlled by ion-exchange, while Sr release was affected primarily by dissolution of the secondary minerals. The later release of K, Al, and Si from the HI-column indicated the additional dissolution of a more crystalline mineral (cancrinite-type). A two-site ion-exchange model successfully simulated the Cs release from the LO-column. However, a three-site ion-exchange model was needed for the HI-column. The study implied that the weathering conditions greatly impact the speciation of the secondary minerals and leaching behavior of sequestrated Sr and Cs.

INTRODUCTION

Radioactive contamination at the Hanford Site in southeastern Washington State, USA has been a well publicized and contentious issue among site operators, academics, regulators and the general public. Of particular concern is leakage of caustic high-level radioactive waste (HLRW) from underground storage tanks into the vadose zone and groundwater aquifer [1-3]. Hanford Site cleanup efforts have focused on removing the caustic HLRW from old storage tanks using various mining and water sluicing processes [4-7]. Of the 149 single shell tanks, approximately 65 to 70 have been diagnosed as having released HLRW to the subsurface either from loss of tank integrity or from pipes used during transfers into and out of the tanks [8]. Various aspects of the acute effects of the released HLRW on sediments, including mineral weathering and contaminant transport have been extensively investigated [9-11].

The behavior of radionuclides in the contaminated sediment after the removal of the caustic source, however, has been rarely studied, especially under unsaturated condition, which is the most realistic scenario of the vadose zone considering the dry climate of Hanford site. Moreover, the behavior of contaminants is strongly affected by multiple compounds in dynamic transport systems, yet most previous studies have focused on the behavior of individual contaminant uptakes with one or two competing compounds using a batch system under saturated condition. Eventually, sediment pore water is expected to return to the circumneutral pH and low ionic strength conditions after a long time elapses, which makes remobilization of the radioactive contaminants sequestered in the impacted sediments possible. Therefore, the release of contaminants from the weathered sediments in which secondary minerals formed during the initial caustic and very saline HLRW fluids interaction with the sediments [5] needs to be investigated with multiple compounds in dynamic transport system under unsaturated conditions that are most representative of the Hanford vadose zone environment.

Previous researchers have identified various types of secondary minerals that sequester contaminants (especially Sr and Cs) during nucleation and crystal growth as a result of contacting

caustic HLRW [9, 12-16]. Zeolites and feldspathoids are the most common secondary minerals observed [17]. The process of secondary mineral formation under such conditions involves transformation from predominantly amorphous to increasingly crystalline phases, i.e., mineral-ripening processes that include nucleation of aqueous aluminosilicate species → amorphous phase → zeolite (linde A) → sodalite → cancrinite (the transformations are not strictly isochemical) [15, 18-20]. Specific characteristics of these secondary minerals have been also extensively studied through experimentation, including chemical composition, molecular structure, thermodynamic parameters, reaction constants, surface area, and ion exchange capacity [15, 18-20]. In spite of these extensive efforts, however, it still remains a challenge to understand the suite of geochemical reactions affecting contaminant release from the weathered sediments because of the diversity of parallel reaction pathways possible over long times during and after the caustic high salinity conditions diminish.

Therefore, in the current work, an inverse modeling approach has been used to elucidate the secondary mineral transformation and metal release based on the results from unsaturated column leaching experiments. The combined modeling and experimental results were intended to identify geochemical controls over contaminant mobility that might occur during reintroduction of fresh background pore water (BPW) following removal of the caustic waste source. The reactive transport code CrunchFlow (www.csteefel.com) was used for this purpose because of its capability to simulate concurrent mineral dissolution, precipitation, sorption, ion exchange, and/or surface complexation reactions and transport [11, 21].

The specific objectives of this study were to 1) identify the reactivity of secondary precipitates containing the sequestered contaminants (Sr and Cs), 2) gain a mechanistic understanding of the coupled reactions linking mineral weathering and contaminant mobility under unsaturated conditions, and 3) develop a model to simulate and verify the hypothesized release mechanisms and the release rates of the contaminants immobilized on or in the secondary minerals. To achieve these specific objectives, unsaturated column leaching experiments were conducted using sediments weathered in the

presence of a caustic waste simulant and then subjected to infusion with simulated BPW. Based on the characterization of the weathered sediments and the data from the column experiments, hypotheses governing the short-term release of multiple contaminants were formulated and tested using the CrunchFlow reactive transport model.

MATERIALS AND METHODS

Preparation and Characterization of the Weathered Sediment. Hanford fine sand was collected from the 218-E-12B burial ground excavation site and used to prepare two weathered sediment conditions representative of "low" and "high" concentrations of Sr and Cs characteristic of caustic HLRW. A brief description of the laboratory weathering process is given below and more details can be found in Chorover et al. (2008) and Thomson et al. (2010) [9, 21]. The air-dried sediments were reacted for six months in the presence of ambient CO_2(g) with a synthetic tank waste leachate (STWL) containing Sr and Cs each at concentrations of either 10^{-5} or 10^{-3} molal (m), hereafter referred to as LO- and HI-conditions, respectively. The STWL composition used in the weathering process is summarized in Table S1 in Supporting Information (SI). After reaction with STWL, sediments were washed repeatedly using ethanol to remove entrained solution, and then freeze dried until further use. Minerals in the weathered sediment were identified using synchrotron x-ray diffraction (XRD) analysis [9, 21]. More detailed information is included in the SI. The laboratory-weathered sediments showed characteristics similar to actual contaminated sediments obtained from locations underlying representative leaking tanks at the Hanford Site [22].

Unsaturated Column Leaching Experiments. Unsaturated columns packed with the weathered sediment were prepared using the "hanging column method" [23]. The details of column setup are also described in the SI. The columns were made of non-reactive acrylic (2.54 cm in diameter and 11.43 cm long) and one tensiometer was placed at the midpoint of each column. Each column was packed with

one of the air-dried, weathered Hanford sediments (LO- or HI-) and initially saturated from the column bottom with BPW. The composition of BPW is given in Table S1. After saturation, additional BPW was dripped onto the top surface of the column, while hanging head pressure (suction) was applied to the bottom of the column using solution-filled Teflon tubing to get optimal water saturation (0.75) in the column based on a previously obtained water-retention curve [24, 25]. A syringe pump was used to achieve a steady-state flow of BPW. After achieving an initial steady-state flow, a nonreactive Br tracer was introduced into the columns with the BPW solution. The Br breakthrough curve was used to determine the dispersivity of each column using numerical optimization with Parameter Estimation and Uncertainty Analysis (PEST) (http://www.pesthomepage.org). The optimization results and the specific parameters of the columns are summarized in Figure S1 and Table S2. Leachate samples were collected daily with a fraction collector using high-density polyethylene bottles to avoid Si contamination. The pH of each effluent sample was measured immediately after collection, and the samples were kept in a refrigerator (at 4°C) until further analysis. Concentrations of dissolved Sr and Cs were analyzed with inductively coupled plasma mass spectrometry (ICP-MS) after filtration with a syringe filter (0.45 μm size). Other selected cations were analyzed using ICP optical emission spectroscopy (OES).

Simulation of the Leaching Behavior of Sr and Cs at Unsaturated Conditions. The reactive transport model, CrunchFlow was employed to simulate the release mechanisms of Sr and Cs. In contrast to our prior study pertaining to saturated transport at long reaction times [16], the simulations in this study only focused on the more complex initial period of elapsed times (< 200 PV) in the leaching experiments. Specific thermodynamic parameters for the minerals were obtained from the literature and the EQ3 database if they were available [12, 18, 21, 26-28]. Unavailable thermodynamic and kinetic parameters were estimated by numerical optimization of the simulation results to the experimental data (see discussion below). Because of the lack of specific mineral information and the unknown value of specific surface areas, mineral reaction rates are presented as $mol_{mineral}\ m^{-3}_{sediment}\ s^{-1}$ rather than as

$mol_{mineral}\ m^{-2}{}_{mineral}\ s^{-1}$ since the latter is only reliable when the specific surface areas of the reacting phases are known [21].

Several assumptions were made before the model construction. The model was based on two major reactions: mineral dissolution/precipitation and ion-exchange. Two target contaminants (Sr and Cs) were assumed to originate solely from the initial weathering process because the concentrations of these two contaminants in the STWL were much higher than these two elements in uncontaminated natural sediments. During the weathering process, the contaminants were considered to be removed from the STWL solution either by coprecipitation into the neoformed secondary minerals or by ion-exchange reactions with the neoformed and native sediment minerals. The relative importance of the release mechanisms, and their associated parameterization (see below) were determined using inverse methods, which involved optimization of specific parameters for ion exchange and mineral dissolution/precipitation rate constants.

RESULTS and DISCUSSION

Characterization of the Secondary Minerals in the Weathered Sediments. Comparison of the XRD patterns of the sediment fine fraction before and after STWL weathering processes revealed the emergence of newly formed precipitates including sodalite and chabazite (Figure 1). The XRD patterns of the LO-sediment showed the representative reflections for sodalite at d-spacing values of 6.32, 3.70, and 2.11 Å (Figure 1b and 1c). The XRD patterns for the HI-sediment instead showed distinct peaks associated with chabazite at d-spacing values of 9.60, 4.27, and 2.93 Å (Figure 1d and 1e). Similar reflections for sodalite and chabazite were not observed in the XRD pattern of native (unweathered) Hanford sediment (Figure 1a). The XRD patterns indicate that the major neoformed secondary minerals formed after the weathering process are sodalite and chabazite for the LO- and HI-sediment, respectively. Sodalite is a feldspathoid mineral, and the formation of feldspathoids as a result of the

weathering of Hanford sediment has been previously reported [9], where the formation follows an Ostwald ripening sequence, beginning with a precursor zeolite followed by transformation to a more crystalline feldspathoid, i.e., sodalite or cancrinite [15, 18-20]. The chabazite observed in the HI-sediment is a zeolite mineral that was also observed to form during incongruent weathering of kaolinite under HI-conditions [10].

Changes resulting from additional reaction with BPW were not evident in the comparison of XRD patterns (i.e., the same minerals were present before and post leaching). However, the intensities of the chabazite reflections in the HI-column decreased after BPW leaching, indicating potential mineral dissolution.

BPW Leachate Results from the Unsaturated Column Experiment. The effluent pH and cation concentrations released from the columns are shown in Figure 2. Effluent Si concentrations in the LO-column (not shown) are similar to those in the HI-column (Figure 2b). The effluent pH in both columns slowly decreased over time from a value above 10 (

Figure 2a and 2d); then leveled off at approximately 7.5 after 80 PV. Decreases in Na, Al (

Figure 2a and 2d), and Cs (

Figure 2b and 2e) concentrations were observed during the initial stages of leaching. However, effluent Cs concentration increased slowly again at later leaching stages (> 120 and > 80 PV for the HI- and LO-columns, respectively). Effluent Si concentration followed a decreasing trend similar to those shown for Na, Al, and pH. Relatively sharp drops in pH, Na, and Si concentrations occurred at approximately 50 PV in the HI-column. However, the concentrations of Sr and other divalent cations (Ca and Mg) remained low in the early stages of leaching until 40 PV and 80 PV for the HI- and LO-columns, respectively (

Figure 2c and 2f). The concentration of K was quite low in both the HI- and LO-column effluents until an abrupt sharp breakthrough of K occurred in the HI-column after 130 PV (Figure 2c). A more gradual breakthrough of K was observed in the LO-column effluent after 100 PV (Figure 2f).

The initially decreasing concentration trends of Na, Al, and Si in the column effluents could be an indication of dissolution of labile aluminosilicate secondary minerals formed during the STWL weathering process [12, 15, 21, 29]. However, identification of the amorphous solid phase or secondary mineral undergoing dissolution is quite challenging because of the transient nature of the labile mineralogy. In addition, some STWL solutes adsorbed on the surface of the secondary minerals may

have readily desorbed or leached out from the weathered sediments at the same time when the weathered sediments in the columns were re-wet during the re-saturation step and subsequent flushing with the BPW, even at the early stage. Thus, we do not postulate the identity of the dissolving mineral phase due to the insufficient information.

Dissolution of neoformed minerals appears to be the major source for the initial release of contaminants and solutes from the weathered sediment. The release of Sr is considered to be dominantly controlled by secondary mineral dissolution [21]. However, the concentrations of Sr found in the HI- (< 40 PV) and LO-columns (< 80 PV) were quite low, indicating the existence of an unspecified reaction or mechanism retaining Sr such as Sr sorption in the weathered sediments [30]. Generally, the breakthrough of Cs release (after the immediate pulse at the start of the leach tests) was much more strongly retarded than that of Sr in both the HI- and LO-columns. An abrupt decrease in Na effluent concentrations occurred at 40 PV in the HI-column and at 80 PV in the LO-column, although the decrease in Na was more evident in the HI-column. Unlike Na and Al, other cations (Ca, Mg, and K) showed increasing concentrations with time similar to breakthrough-like-profiles, but their effluent curves exhibited more monotonically and slowly increasing trends compared to a classical breakthrough profile. Monovalent and divalent cations also showed different effluent concentration profiles in the HI-column. The breakthrough of divalent cations (Ca, Mg, and Sr) began at the precise moment (about 40 PV) that Na started to decrease, while breakthrough of monovalent cations (Cs and K) did not occur until approximately 130 PV (

Figure 2b and 2c) in the HI-column. The breakthrough of all metal cations in the LO-column appeared to start at the same time when the effluent Na decreased rapidly at about 80 PV, although the monovalent ions (Cs and K) showed very gradual breakthrough (Figure 2e and 2f).

The breakthrough profiles of metal cations suggest ongoing ion-exchange reactions in the column sediments. As described below, CrunchFlow modeling suggests that the breakthrough of a given cation began when available ion-exchange sites in the sediments approached equilibrium with respect to that specific cation. The ion-exchange sites in the HI- and LO-sediment are not equivalent, since alteration of ion-exchange behavior on sediment is induced by variation in the hyperalkaline weathering processes [31] and the composition of neoformed minerals depending on Cs and Sr concentrations present in the STWL. Hence, variations in weathering conditions are likely to change the density and selectivity coefficients of ion-exchange sites in the reacted sediments [11, 21, 32]. Selectivity within and between ion-valences is also related to ion hydration energy. Extended x-ray

absorption fine structure (EXAFS) studies have shown that cations with different hydration energies vary in their affinity for ion-exchange sites [11, 33].

The major Sr breakthrough found at about 40 PV of the HI-column was controlled by an ion-exchange reaction. An additional minor breakthrough of Sr also occurred at 130 PV only in the HI-column (

Figure 2b), accompanied by breakthroughs of Cs, K, and Si (Figure 2b, 2c) and Al (Figure S2). The increase in Si and Al concentrations at the later stage was probably due to slow dissolution of more crystalline aluminosilicate minerals, such as cancrinite [$Na_6Ca_2Al_6Si_6O_{24}(CO_3)_2$]. Many researchers have reported the formation of cancrinite as a secondary mineral in caustic conditions similar to our weathering process [12, 15, 31]. In addition, cementitious Al and Si end-products have been found as secondary minerals in hyperalkaline high ionic strength environments [21, 34].

Although saturation degree of the columns was 0.75, concentrations of Cs and Sr in early period (< 120 PV) of the HI-column were not significantly different from those measured for saturated conditions (Figure S3). There was, however, more release of Cs from the saturated column than from the unsaturated column. The LO-column also showed some delay in Sr and Cs releases under unsaturated column relative to saturated conditions.

Modeling for Cation Release and Mineral Dissolution Reactions. Based on the XRD analyses, a chabazite-type zeolite or a sodalite-type feldspathoid containing Sr and Cs was incorporated in the model. Both of these minerals were susceptible to dissolution due to under-saturation of solution with respect to these phases upon introduction of BPW. The relative amounts of zeolite and feldspathoid present in the weathered sediments varied depending on the weathering conditions. Total zeolite mass was limited to 5 wt% of feldspathoid in the LO-sediment, and 5 wt% zeolite in the HI-sediment was considered as feldspathoid to accommodate XRD observations and the known ripening process [19, 20]. In the HI-sediment, strontianite ($SrCO_3$) observed in EXAFS analysis (Table S3) was included as another Sr sequestering source, because strontianite has been reported to sequester Sr (Table S3) [9, 34].

No $SrCO_3$ precipitate was found in the LO-sediment. Calcite amount was calculated as 5.7 wt% in the LO-sediments and negligible amount (0.001 wt%) in HI-sediment, respectively.

The masses of Sr and Cs in the weathered sediments were determined by sequential extraction experiments. More details for the method are found in Thomson et al. (2010) [21]. Sr and Cs contents in the HI-sediment were $4.1x10^{-5}$ and $3.3x10^{-6}$ mol/g sediment, and those in the LO-sediment were $4.7x10^{-6}$ and $9.9x10^{-8}$ mol/g sediment, respectively. The distribution of Sr and Cs among the secondary minerals (feldspathoid and chabazite) was different depending on the weathering conditions. In addition, the dissolution reaction rate of each secondary mineral in the weathered sediments was varied due to the various combined structure of Sr or Cs despite the same type of minerals being present in the weathered sediments [34]. The distribution ratio of the contaminants and the kinetic reaction rates for the dissolution of the secondary minerals were determined by numerical optimization of simulation predictions to the experimental column effluent data. The optimized constants for the reaction rates of the secondary minerals are summarized in Table 1. The simulated results for cation releases from the weathered sediments under unsaturated conditions are also shown in Figure 2 as the solid lines in comparison to the measured data (symbols). The constructed model reasonably well simulated the dynamic transport behavior of released cations such as the Na plunge, sequential emergence of multiple cations, and the general behavior of Sr and Cs releases.

Simulation of contaminant release was initially tested using a single reaction, either mineral dissolution or ion-exchange, but the results were not satisfactory. After several trial and error approaches, the acceptable result for Sr release was simulated by mineral dissolution with a minor contribution from ion-exchange. However, Cs release behavior was best described using mostly ion-exchange reaction with a minor contribution of mineral dissolution. The best simulation for leachable Sr in the HI-column was obtained using a distribution of feldspathoid (23 wt%), strontianite (32 wt%), and zeolite (45 wt%) with a 1 mol Sr/mol mineral stoichiometric ratio. However, the optimum distribution of leachable Sr in the LO-column was 30 wt% in zeolite with a 1 mol Sr/mol mineral ratio,

and 70 wt% in feldspathoid with a 0.2 mol Sr/mol mineral ratio to honor the estimated formation ratio of the secondary minerals (5 wt% and 95 wt% for zeolite and feldspathoid, respectively). On the other hand, 35 wt% of the leachable Cs was simulated in zeolite with a 2 mol Cs/mol mineral ratio in both the HI- and LO-columns. Finding only minor incorporation of Cs into the neoformed secondary minerals was also experimentally observed previously [9].

The optimized inverse simulation results confirmed the hypothesis made before the modeling was performed. The hypothesis was that most of leachable Sr was removed from STWL by the secondary minerals formed during the initial weathering process, while only a small portion of the leachable Cs was sequestered in the process of secondary minerals formation. The rest of the leachable Cs was considered to be present on ion-exchange sites in either native sediments or the neoformed solid phases. Ion-exchange processes are also suggested to be the dominant mechanism controlling the Cs release in the Hanford sediment [11, 21, 32].

Modeling of Ion-Exchange Reactions. Various types of ion-exchange models have been suggested to predict Cs sorption/desorption behavior in the Hanford Site subsurface environment. Previously applied ion-exchange reactions with modeling conditions similar to this research are summarized in Table S4. Zachara et al. (2002) proposed two types of sites for the modeling of Cs sorption; planar and frayed edge site (FES) [32]. They determined the total number of sites and the partitioning between these two selected sites by conducting an independent CEC measurement [35]. Steefel et al. (2003) used those two types of exchange sites, but further split the FES into strong and weak sites; i.e., three exchange sites (planar, FES1, FES2) [11]. They used various methods for CEC measurement, including the method used by Zachara et al. [36]. Thompson et al. [21] used the ion-exchange conceptual model developed by Steefel et al. (2003) with adjusted parameters, including independently determined CEC [37]. In spite of the different approaches, the applied Cs ion exchange models all agree on the relative amount and characteristics of the FES vs. planar ion-exchange sites in the weathered sediment (i.e., a small portion of FES with a strong affinity could sequester most of the Cs during the weathering

process, while the total CEC is dominated by planar sites whose affinity for Cs adsorption is relatively weak).

The previous ion-exchange models were commonly constructed based on the experiments under saturated condition either using batch and/or column system. However, the natural condition in vadose zone, especially of Hanford site, more closely resembles the unsaturated condition. In addition, some models considered limited numbers of selected cation species of interests for the simulation of ion-exchange reactions. In a more realistic scenario, multiple cation species released from various sources are expected to compete simultaneously for the possible ion-exchange sites, and their interrelated behavior also has to be considered.

In this study, the previous model schemes were initially applied with proper modification for Sr and Cs releases under unsaturated condition. However, the initial results of simulation using previous models did not agree with the experimental results, especially considering multiple species simultaneously. Thus, the concept of two types of ion-exchange sites (planar and FES) was only introduced from the initial modeling attempts. In addition, considering different extents of alteration in the sediments during the weathering process, two types of planar sites (planar 1 and planar 2 sites) in which selectivity is different for mono- and divalent cations were proposed for the HI-sediment. Alteration in types of cation exchange site and affinity by weathering processes has been also suggested previously [31].

The number of ion-exchange sites that sum to the total CEC ($mmol_c\,kg^{-1}$) and the selectivity coefficient for each site were determined by numerical optimization using CrunchFlow to obtain the best describing result to the measured leaching data (Table 2). The total optimized CEC value was 158.17 $mmol_c\,kg^{-1}$ for both HI- and LO-sediments. The total CEC value is greater than the previously reported CEC values for Hanford Site unreacted sediment, which range from 36 to 125.2 $mmol_c\,kg^{-1}$ [11, 21, 30, 32]. However, the optimized CEC value of weathered sediments is still compatible with the calculated CEC based on eluted cation concentrations of Ca, Mg, and K, which indicate approximately

142 $mmol_c\,kg^{-1}$ for LO- and 163 $mmol_c\,kg^{-1}$ for HI-sediments (See the calculation details in the SI). The high optimized CEC value is attributed to additional sites in the weathered sediment, especially associated with neoformed minerals. It may also indicate that a fraction of the sites (potentially zeolite framework sites) are inaccessible for Co(III)-hexamine used in the Cohex method [37] but accessible for Ca, Mg and K cations. As a result, the amount of available ion exchange sites by the optimization process was higher than the previous value measured using the Cohex method [16].

The release of K after 130 PV of leaching in the HI-column was underestimated by the optimized prediction model (Figure 2c), while the behavior of Sr and Cs release during this leaching period was successfully simulated with the optimized ion-exchange conceptual model presented here. The additional release of K suggests a potential for additional mineral dissolution, such as the more crystalline cancrinite or other minerals present in the Hanford weathered sediment that contain K, even though a process is not represented in the CrunchFlow optimized prediction. The slow dissolution of more crystalline minerals in the later stages of leaching is consistent with the hypothesis discussed earlier that mineral-ripening processes occur during the weathering process, resulting in the formation of more stable solids that likely dissolve more slowly. However, unfortunately, no specific information on slowly dissolving more crystalline minerals is available now to be added to the reaction network.

ENVIRONMENTAL IMPLICATIONS

Inverse modeling results showed that the initial weathering conditions greatly affected the major aspects of the leaching behavior of multiple cations beyond anticipation; the key parameters were the secondary mineral composition and the ion-exchange characteristics. Identification and quantification of the less crystalline zeolite, which is believed to be as an unstable or labile secondary mineral in the early stages of leaching, are greatly challenging to obtain by spectroscopic and microscopic analyses, but critical to understand the behavior of contaminant release. Application of the inverse conceptual

modeling combined with the realistic column leaching tests demonstrated the applicable indirect assessment of the secondary mineral formed through the mineral transformation process. Although the release behaviors of Cs and Sr from the weathered Hanford vadose sediments were expected to vary depending on the types of contaminants and weathering processes, better understanding of the types of individual secondary minerals and amorphous precursor minerals as well as their dissolution rate, total number, and cation selectivity attributes of ion exchange sites are required to predict the release of Sr and Cs from the contaminated Hanford sediments.

ACKNOWLEDGMENTS

Funding was provided for this research by the U.S. Department of Energy's Subsurface Biogeochemical Research (SBR) Program, Contract No. DE-FG02-06ER64190 and No. DE-AC02-05CH11231. Portions of this research were supported through a Cooperative Agreement (DEFC09-07-SR22506) between The Department of Energy and The University of Georgia Research Foundation. Additional funding was supported by WCU(World Class University) program at the Division of Advanced Nuclear Engineering (DANE) in POSTECH through the National Research Foundation of Korea funded by the Ministry of Education, Science and Technology (R31 - 30005). Synchrotron XRD analysis was carried out at the Stanford Synchrotron Radiation Lightsource, a national user facility operated by Stanford University on behalf of the U.S. Department of Energy, Office of Basic Energy Sciences.

REFERENCES

1. Zachara, J. M.; Serne, J.; Freshley, M.; Mann, F.; Anderson, F.; Wood, M.; Jones, T.; Myers, D., Geochemical processes controlling migration of tank wastes in Hanford's vadose zone. *Vadose Zone J.* **2007,** *6*, (4), 985-1003.
2. Department of Energy, *Closing the Circle on the Splitting of the Atom: The Environmental Legacy of Nuclear Weapons Production in the United States and What the Department of Energy is Doing About It*. U.S. Department of Energy: Washington, DC, 1995; Vol. DOE/EM-0266.
3. Ahearne, J. F., Radioactive waste: the size of the problem. *Phys. Today* **1997,** *50*, 24-29.
4. Nash, K. L.; Borkowski, M.; Hancock, M.; Laszak, I., Oxidative Leaching of Plutonium from Simulated Hanford Tank-Waste Sludges. *Separ. Sci. Technol.* **2005,** *40*, 1497-1512.
5. Bond, A. H.; Nash, K. L.; Gelis, A. V.; Sullivan, J. C.; Jensen, M. P.; Rao, L., Plutonium Mobilization and Matrix Dissolution during Experimental Sludge Washing of Bismuth Phosphate, Redox, and Purex Waste Simulants. *Separ. Sci. Technol.* **2001,** *36*, (5&6), 1241-1256.
6. Hallen, R. T.; Geeting, J. G. H.; Lilga, M. A.; Hart, T. R.; Hoopes, F. V., Assessment of the Mechanisms for Sr-90 and TRU Removal from Complexant Containing Tank Waste at Hanford. *Separ. Sci. Technol.* **2005,** *40*, 171-183.
7. Wilmarth, W. R.; Rosencrance, S. W.; Nash, C. A.; Edwards, T. B., Sr/TRU Removal from Hanford High Level Waste. *Separ. Sci. Technol.* **2001,** *36*, (5&6), 1283-1305.
8. U.S. DOE, *Draft Tank Closure and Waste Management Environmental Impact Statement for the Hanford Site*. Office of Environmental Management: Richland, WA, 2009; Vol. DOE/EIS-00391-Draft.
9. Chorover, J.; Choi, S.; Rotenberg, P.; Serne, R. J.; Rivera, N.; Strepka, C.; Thompson, A.; Mueller, K. T.; O'Day, P. A., Silicon control of strontium and cesium partitioning in hydroxide-weathered sediments. *Geochim. Cosmochim. Acta* **2008,** *72*, (8), 2024-2047.
10. Serne, R. J.; Zachara, J.; Burke, D., Chemical information on tank supernatants, Cs adsorption from tank liquids onto Hanford sediments and field observations of Cs migration from past tank leaks. *Pacific Northwest National Laboratory* **1998,** *PNNL-11495*.
11. Steefel, C. I.; Carroll, S.; Zhao, P. H.; Roberts, S., Cesium migration in Hanford sediment: a multisite cation exchange model based on laboratory transport experiments. *J. Contam. Hydrol.* **2003,** *67*, (1-4), 219-246.
12. Deng, Y.; Flury, M.; Harsh, J. B.; Felmy, A. R.; Qafoku, O., Cancrinite and sodalite formation in the presence of cesium, potassium, magnesium, calcium and strontium in Hanford tank waste simulants. *Appl. Geochem.* **2006,** *21*, (12), 2049-2063.
13. Bickmore, B. R.; Nagy, K. L.; Young, J. S.; Drexler, J. W., Nitrate-cancrinite precipitation on quartz sand in simulated Hanford tank solutions. *Environ. Sci. Technol.* **2001,** *35*, (22), 4481-4486.
14. Chorover, J.; Choi, S. K.; Amistadi, M. K.; Karthikeyan, K. G.; Crosson, G.; Mueller, K. T., Linking cesium and strontium uptake to kaolinite weathering in simulated tank waste leachate. *Environ. Sci. Technol.* **2003,** *37*, (10), 2200-2208.
15. Qafoku, N. P.; Ainsworth, C. C.; Szecsody, J. E.; Bish, D. L.; Young, J. S.; McCready, D. E.; Qafoku, O. S., Aluminum Effect on Dissolution and Precipitation under Hyperalkaline Conditions: II. Solid Phase Transformations. *J. Environ. Qual.* **2003,** *32*, 2364–2372.
16. Choi, S.; Crosson, G.; Mueller, K. T.; Seraphin, S.; Chorover, J., Clay mineral weathering and contaminant dynamics in a caustic aqueous system: II. Mineral transformation and microscale partitioning. *Geochim. Cosmochim. Acta* **2005,** *69*, (18), 4437-4451.
17. Um, W.; Serne, R. J.; Yabusaki, S. B.; Owen, A. T., Enhanced radionuclide immobilization and flow path modifications by dissolution and secondary precipitates. *J. Environ. Qual.* **2005,** *34*, 1404-1414.
18. Linares, C. F.; Sa´nchez, S.; de Navarro, C. U.; Rodrı´guez, K.; Goldwasser, M. R., Study of cancrinite-type zeolites as possible antacid agents. *Microporous Mesoporous Mater.* **2005,** *77*, 215–221.

19. Scheckel, K. G.; Scheinost, A. C.; Ford, R. G.; Sparks, D. L., Stability of layered Ni hydroxide surface precipitates - a dissolution kinetics study. *Geochim. Cosmochim. Acta* **2000,** *64*, 2727-2735.
20. Ainsworth, C. C.; Pilon, J. L.; Gassman, P. L.; Vandersluys, W. G., Cobalt, cadmium and lead sorption to hydrous iron oxide - residence time effect. *Soil Sci. Soc. Am. J.* **1994,** *58*, 1615-1623.
21. Thompson, A.; Steefel, C. I.; Perdrial, N.; Chorover, J., Contaminant desorption during long-term leaching of hydroxide-weathered Hanford sediments. *Environ. Sci. Technol.* **2010,** *44*, (6), 1992-1997.
22. McKinley, J. P.; Zachara, J. M.; Gassman, P. L.; Ainsworth, C. C.; Arey, B.; McKinley, S.; Schaef, T.; Smith, S. C.; Kimberling, J.; Bish, D. L.; Chipera, S. J.; Snow, P., S-SX SITE MINERALOGY. In *Field Investigation Report for Waste Management Area S-SX*, U.S. Department of Energy, Office of River Protection: Richland, Washington, 2002; Vol. 1, pp 505-528.
23. Dane, J. H.; Hopmans, J. W., Water retention and Storage: Laboratory. In *Methods of Soil Analysis, Part 4, Physical Methods.*, Dane, J. H.; Topp, G. C., Eds. Soil Science Society of America, Inc.: Madison, Wisconsin, 2002.
24. Cherrey, K. D.; Flury, M.; Harsh, J. B., Nitrate and colloid transport through coarse Hanford sediments under steady state, variably saturated flow. *Water Resour. Res.* **2003,** *39*, (6), 1165.
25. Rod, K. A.; Um, W.; Flury, M., Transport of strontium and cesium in simulated Hanford tank waste leachate through quartz sand under saturated and unsaturated flow. *Environ. Sci. Technol.* **2010,** *44*, (21), 8089-8094.
26. Wolery, T. J., EQ3/6, A Software Package for Geochemical Modeling of Aqueous Systems : Package Overview and Installation Guide (Version 7.0). In *A Software Package for Geochemical Modeling of Aqueous Systems: Package Overview and Installation Guide*, Version 7.0 ed.; Lawrence Livermore National Laboratory: Livermore, 1992; pp UCRL-MA--110662.
27. Blanc, P.; Lassin, A., EQ3, Thermoddem. In EQ3, Thermoddem, BRGM institute: 2008.
28. Cole, D., Isotopic exchange in mineral-fluid systems. IV. The crystal chemical controls on oxygen isotope exchange rates in carbonate-H_2O and layer silicate-H_2O systems. *Geochim. Cosmochim. Acta* **2000,** *64*, (5), 921- 931.
29. La Iglesia, A.; Franco, E.; Pozzuoli, A., Stability Diagrams Of Zeolites .2. Phillipsite And Chabazite From Pyroclastic Rocks In Southern Italy. *Neues Jahrb. Mineral. Abh.* **1991,** *162*, 261-280.
30. McKinley, J. P.; Zachara, J. M.; Smith, S. C.; Liu, C., Cation exchange reactions controlling desorption of $^{90}Sr^{2+}$ from coarse-grained contaminated sediments at the Hanford site, Washington. *Geochim. Cosmochim. Acta* **2007,** *71*, (2), 305.
31. Mon, J.; Deng, Y. J.; Flury, M.; Harsh, J. B., Cesium incorporation and diffusion in cancrinite, sodalite, zeolite, and allophane. *Microporous Mesoporous Mater.* **2005,** *86*, (1-3), 277-286.
32. Zachara, J. M.; Smith, S. C.; Liu, C. X.; McKinley, J. P.; Serne, R. J.; Gassman, P. L., Sorption of Cs^+ to micaceous subsurface sediments from the Hanford site, USA. *Geochim. Cosmochim. Acta* **2002,** *66*, (2), 193-211.
33. Kemner, K. M.; Hunter, D. B.; Bertsch, P. M.; Kirkland, J. P.; Elam, W. T., Determination of the site-specific binding environments of surface sorbed cesium on clay minerals by Cs-EXAFS. *J. Phys. IV* **1997,** *7*, 777– 779.
34. Choi, S.; O'Day, P. A.; Rivera, N. A.; Mueller, K. T.; Vairavamurthy, M. A.; Seraphin, S.; Chorover, J., Strontium speciation during reaction of kaolinite with simulated tank-waste leachate: Bulk and microfocused EXAFS analysis. *Environ. Sci. Technol.* **2006,** *40*, (8), 2608-2614.
35. Turner, G. D.; Zachara, J. M.; McKinley, J. P.; Smith, S. C., Surface-charge properties and UO_2^{2+} adsorption of a subsurface smectite. *Geochim. Cosmochim. Acta* **1996,** *60*, 3399–3414.
36. Appelo, C. A. J., Multicomponent ion exchange and chromatography in natural systems. In *Reactive Transport in Porous Media. Reviews in Mineralogy*, Lichtner, P. C.; Steefel, C. I.; Oelkers, E. H., Eds. 1996; Vol. 34, pp 193– 227.
37. Ciesielski, H.; Sterckeman, T., Determination of cation exchange capacity and exchangeable cations in soils by means of cobalt hexamine trichloride. Effects of experimental conditions. *Agronomie* **1997,** *17*, 1-7.

38. Buhl, J. C.; Löns, J., Synthesis and crystal structure of nitrate enclathrated sodalite $Na_8[AlSiO_4]_6(NO_3)_2$. *J. Alloy. Compd.* **1996,** *235*, 41-47.
39. Alberti, A.; Galli, E.; Vezzalini, G.; Passaglia, E.; Zanazzi, P. F., Position of Cations and Water-Molecules in Hydrated Chabazite - Natural and Na-Exchanged, Ca-Exchanged, Sr-Exchanged and K-Exchanged Chabazites. *Zeolites* **1982,** *2*, 303-309.

Table 1. Summarized results of numerical optimization regarding mineral species in the model.

Mineral	HI-sediment		LO-sediment	
	Distribution of Sr (or Cs)	Log (reaction rate) ($mol_{mineral}m^{-3}{}_{sediment}s^{-1}$)	Distribution of Sr (or Cs)	Log (reaction rate) ($mol_{mineral}m^{-3}{}_{sediment}s^{-1}$)
Feldspathoid-Sr	0.23 (Sr)	-4.54	0.70 (Sr)	-5.04
Strontianite	0.32 (Sr)	-4.79		
Zeolite-Sr	0.45 (Sr)	-9.15	0.30 (Sr)	-9.15
Zeolite -Cs	0.35(Cs)	-10.55	0.35(Cs)	-10.55
Zeolite		-9.37		-9.37
Calcite		-5.65		-5.65

Table 2. Summarized results of numerical optimization regarding the ion-exchange reaction in the current model.

Column	type	CEC ($mmol_c kg^{-1}$) (portion)	Exchange reaction	Log K
HI-	Site1 (planar1)	137 (86.6%)	$NaX1 + Cs^+ = Na^+ + CsX1$	0.8
			$SrX1_2 + 2Cs^+ = Sr^{2+} + 2CsX1$	1.42
			$CaX1_2 + 2Cs^+ = Ca^{2+} + 2CsX1$	2.15
			$MgX1_2 + 2Cs^+ = Mg^{2+} + 2CsX1$	2.15
	Site 2 (planar2)	20.6 (13.0%)	$NaX2 + Cs^+ = Na^+ + CsX2$	1.4
			$KX2 + Cs^+ = K^+ + CsX2$	0.08
	Site 3 (edge)	0.572 (0.4%)	$NaX3 + Cs^+ = Na^+ + CsX3$	4.5
			$KX3 + Cs^+ = K^+ + CsX3$	3.0
LO-	Site 1 (planar)	157.6 (99.6%)	$NaX1 + Cs^+ = Na^+ + CsX1$	1.0
			$KX1 + Cs^+ = K^+ + CsX1$	0.5
			$SrX1_2 + 2Cs^+ = Sr^{2+} + 2CsX1$	1.55
			$CaX1_2 + 2Cs^+ = Ca^{2+} + 2CsX1$	2.8
			$MgX1_2 + 2Cs^+ = Mg^{2+} + 2CsX1$	2.8
	Site 2 (edge)	0.572 (0.4%)	$NaX2 + Cs^+ = Na^+ + CsX2$	8.5
			$KX2 + Cs^+ = K^+ + CsX2$	5.25

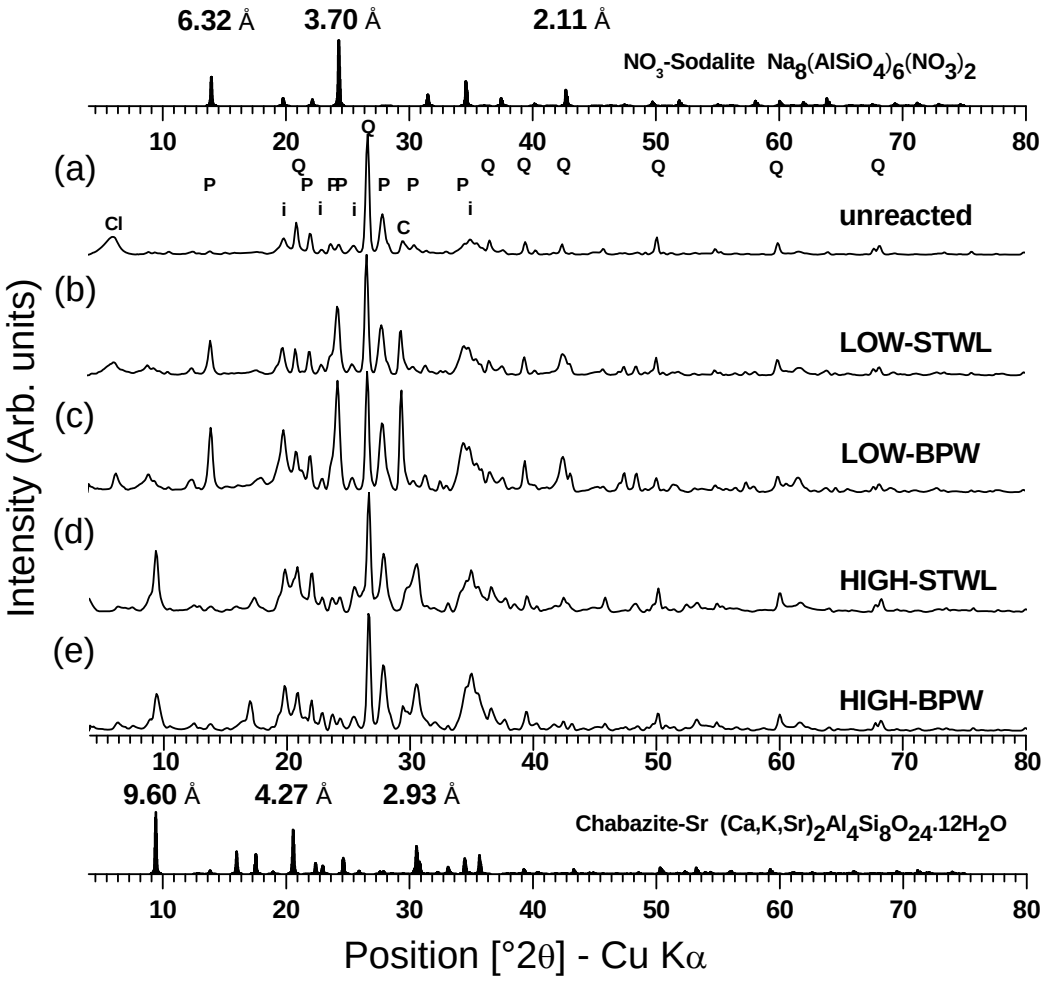

Figure 1. X-ray diffractograms of the fine fractions of the a) unreacted sediment, b) LO-sediment, c) LO-column leached, d) HI-sediment, e) HI-column leached. The top panel represents the diffractogram of a typical NO_3-sodalite [38] and the bottom panel the typical diffractogram of a Sr-rich chabazite [39]. Labels corresponding to the main reflections in (a) are as follows Cl: chlorite, P: plagioclase, i: illite, Q: quartz and C: calcite.

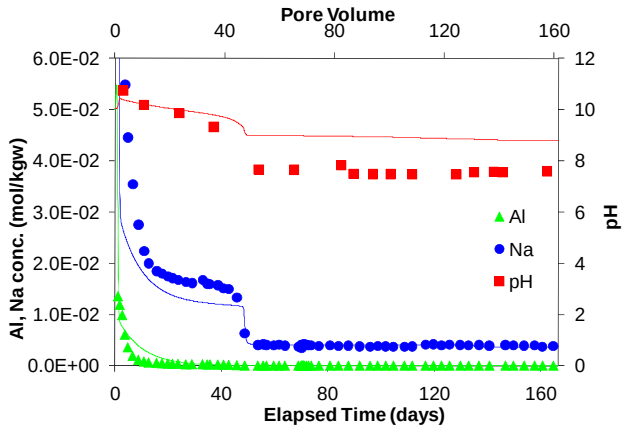

(a) pH, Na, Al in HI

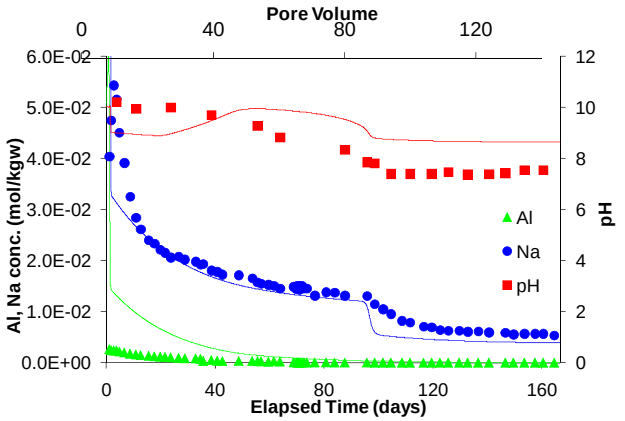

(d) pH, Na, Al in LO

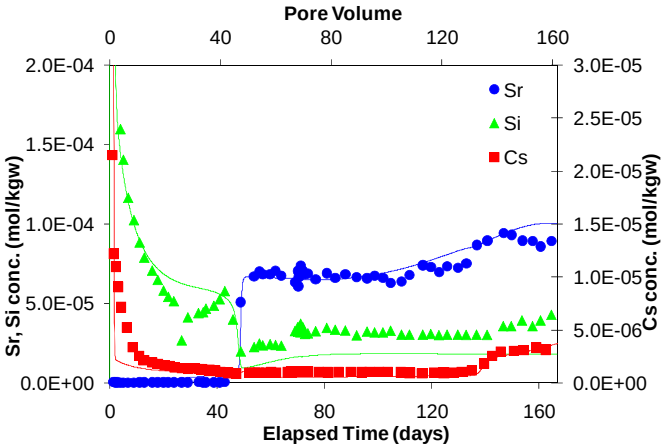

(b) Sr, Cs, Si in HI

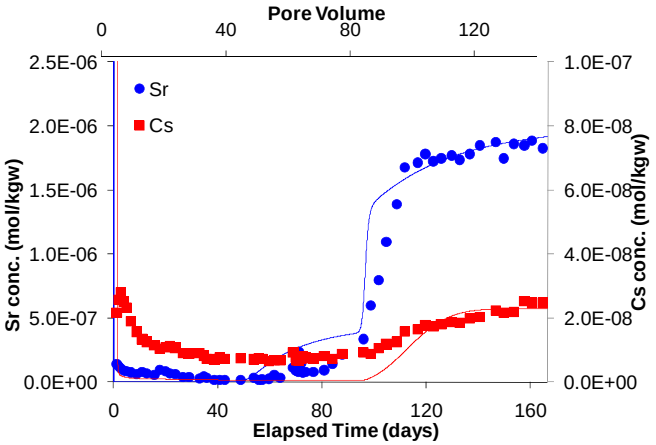

(e) Sr, Cs in LO

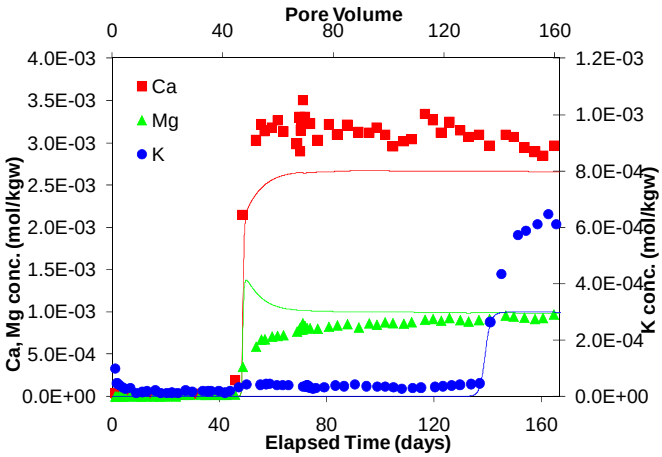

(c) Ca, Mg, K in HI

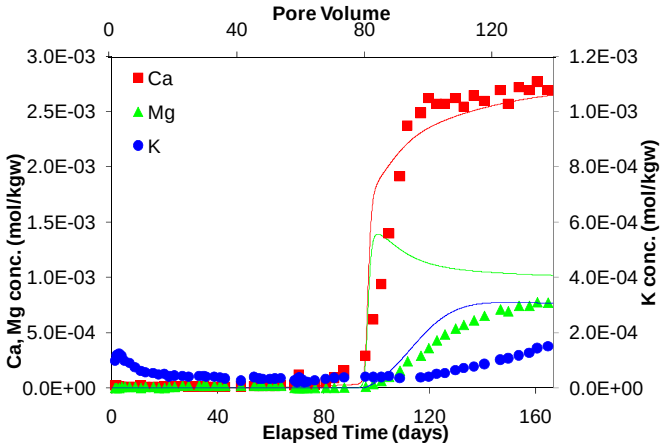

(f) Ca, Mg, K in LO

Figure 2. pH and concentrations of released cations from HI- and LO-sediment in unsaturated condition (symbols: experimental data; lines: model simulation).

Table of contents (TOC) Art